Journal of Physics: Conference Series

PAPER • OPEN ACCESS

Optimization on the mechanical parameters and impact of welding parameters of pulsed TIG welding of Aluminium-Zinc-Magnesium alloy

To cite this article: Prasanth Ponnusamy *et al* 2023 *J. Phys.: Conf. Ser.* **2603** 012039

View the article online for updates and enhancements.

You may also like

- A review on TIG cladding of engineering material for improving their surface property
Kaushik Biswas and Chinmaya Kumar Sahoo
- Post-weld friction stir processing of AA5083-F TIG welds with scandium added fillers
R Aarthi and K S Vijay Sekar
- Effect of shielding gas composition and activating flux on the weld bead morphology of the P91 ferritic/martensitic steel
R S Vidyarthy and D K Dwivedi

This content was downloaded from IP address 103.224.33.130 on 23/07/2024 at 07:22

Optimization on the mechanical parameters and impact of welding parameters of pulsed TIG welding of Aluminium-Zinc-Magnesium alloy

Prasanth Ponnusamy[1], Pon.Maheskumar[2], Mohanraj A[3], Pradeep G M[4], Nanthakumar S[5], Sk Hasane Ahammad[6], Girimurugan R[7*]

[1]Department of Mechanical Engineering, Tagore Institute of Engineering and Technology, Salem, Tamilnadu, India

[2]Department of Mechanical Engineering, Nandha College of Technology, Perundurai, Tamilnadu, India

[3]Department of Mechanical Engineering, K S R Institute for Engineering and Technology, Tiruchengode, Tamilnadu, India

[4]Department of Mechanical Engineering, Velammal Institute of Technology, Chennai, Tamilnadu, India

[5]Department of Mechanical Engineering, PSG Institute of Technology and Applied Research, Coimbatore, Tamilnadu, India

[6]Department of Electronics and Communication Engineering, Koneru Lakshmaiah Education Foundation, Vaddeswaram, Andhra Pradesh, India

[7]Department of Mechanical Engineering, Nandha College of Technology, Perundurai, Tamilnadu, India

*Email: dr.r.girimurugan@gmail.com

Abstract. As a function of pulsed Tungsten Inert Gas (TIG) weld processing factor, authors have studied the relationship between dilution and mechanical qualities including impact toughness, notch tensile strength, hardness in the as-welded condition. Welds made with a pulsed TIG torch have a minimum notch tensile strength and impact toughness than the base metal (BM) because of the grains of the inter-dendritic network formed during the welding process. Weldments made from heat-treatable (Al-Zn-Mg) Aluminium alloys have their process parameters for pulsed TIG welding optimized employing the Taguchi analysis to get the best possible mechanical qualities. Notch tensile strength is shown to be inversely proportional to impact toughness.

Keywords: Impact toughness, Aluminum alloy, hardness, notch tensile strength, pulsed TIG welding.

1. Introduction

The aerospace and defense industries make extensive use of alloys containing Aluminum, Magnesium, and Silicon [1]. Arc welding, like tungsten inert gas (TIG) welding, involves striking a molten pool of

Content from this work may be used under the terms of the Creative Commons Attribution 3.0 licence. Any further distribution of this work must maintain attribution to the author(s) and the title of the work, journal citation and DOI.
Published under licence by IOP Publishing Ltd

metal with a spark from a disposable electrode. The TIG welding technique is commonly used to join these metals together [2]. TIG welding employs a pulsing process with magnetic arc oscillation. One post-weld heat treatment can artificially age the weld, the HAZ, and the parent metal if all three are in solution, have been heat-treated, and are in an ageing condition. Since the base metal (BM) is only slightly diluted into the weld, it is difficult to obtain desirable properties in the as-welded state, especially strength and toughness [3-5]. There are several methods for enhancing grain refinement at the weld zone. These include dilution, surface nucleation, and inoculation with heterogeneous nucleates. While inoculation can be used to improve the fusion zone during casting, it is ineffective when welding. The surface nucleation approach also failed to gain traction because to the difficulty of its setup and operation [6-7]. The term "welding" refers to the process of permanently attaching two or more materials together by applying heat and, in certain cases, pressure to the joint [8-10]. By melting the faying pieces to be joined and then hardening the molten metal, a permanent junction is generated with strength equal to or greater than the parent metal [11-12]. The use of filler material during welding is optional and is determined by the thickness of the metal sheets being welded together [13-14]. Because welding involves so many changes in so many material characteristics, the welding ability of any material to be connected is mostly dependent on the metallurgical event occurring during welding. Aerospace, spacecraft, structural, and military sectors all favour aluminium alloys [15-18]. Aluminum alloys offer improved properties in a variety of areas, including elasticity, strength, toughness, and corrosion resistance. [19-20]. 6061 Strength can be improved in heat-treatable Aluminium Alloy 6061 through a process called precipitation hardening, and a phase transition also happens when welding is performed at high temperatures [21]. For Tungsten Inert Gas (TIG) welding, a non-consumable electrode and parent metal are used to form an arc that heats the faying metals during coalescence. [22-23]. In order to combine Aluminium Alloy 6061, TIG welding is the most common method. Pulsing and magnetic arc oscillations are just two of the various ways used in the TIG joining process. TIG welding has been used extensively for a wide variety of aluminium [24]. Pulsed tungsten inert gas welding of thick plates (with a thickness of 6 mm) of aluminium alloys was investigated [25]. The shear strength was shown to be influenced by pulse current and porosity in the weld zone. Although the shear strength of the source metals was 85 MPa, the shear strength of the weld junction was only 73 MPa. With the goal of controlling the welding speediness for a satisfactory welded joint, authors [26-27] looked into the instinctive tungsten inert gas welding of Aluminium Alloy 5083 with a filler rod of Aluminium Alloy 5356. This study aims to apply the Taguchi approach to the practice of pulsed TIG welding in order to establish the optimum amount of base metal to utilize while diluting the weld pool. Pulsed current has been shown to have many positive effects in metalworking, including narrowing the HAZ, improving grain refinement in the fusion zone, decreasing distortion, lowering the sensitivity to hot cracking, preventing segregation, and decreasing residual stresses. Refining the grain structure with pulsing and magnetic arc oscillation reduces the heat-treatable alloy's susceptibility to hot cracking. Filler metals with refining components are often used in fusion zones, but diluting the base metal can achieve the same result. Since dilution can reduce hot cracking susceptibility and improve mechanical characteristics in heat-treatable alloys, it is especially important in these materials.

2. Experimental procedure

Aluminum-Zinc -Magnesium was used as the base metal, and Aluminum alloy 5128 was used as the filler material. Table 1 provides a catalogue of available base and filler compounds. When deciding on a filler material, it is important to take the weld's mechanical qualities and the material's susceptibility to cracking into account.

Table 1. Base and filler material chemical composition (weight percentage)

Material	Mg	Si	Cu	Cr	Mn	Zn	Ti	Al
Al-Zn-Mg alloy (base)	2.24	0.02	0.22	0.06	0.32	6.20	0.05	Balance

Aluminium alloy 5128 (filler)	5.0	0.20	0.15	0.10	0.50	0.25	0.10	Balance

For these weld tests, authors used an AC welding machine with a 380-W power output. Base current, peak current, pulse frequency, and welding speed are all factors in the quality management of pulsed TIG welding. The results of our investigation into the relationship between dilution and mechanical characteristics and processing variables are presented below. In the previous research, numerous process parameters were altered to examine their impact on various aspects of weld quality. These included the shielding gas flow rate and the placement of the backup plate. While maintaining all other aspects of the procedure, authors changed just one of them throughout the pilot runs. Full penetration of the beads was observed, and the ideal value of base current, peak current, and pulse frequency was discovered. Tables 2 and 3 display the range of the process variables and the constants used in this analysis, respectively. This study optimized the process variables for maximum mechanical properties using the Taguchi technique. In this investigation, authors focused on four distinct process factors over two distinct levels for each. There are a total of seven degrees of freedom, due to the interplay between the four parameters. So, in this research work 8 levels of (L8) orthogonal arrays were chosen. To minimize the impacts of noise and error, authors conduct each condition twice. Table 4 lists the specifics of the chosen orthogonal array.

Table 2. Factors and its level

Process variable	Symbol	Minimum level (1)	Maximum level (2)
Peak current (Amps)	A	70	80
Base current (Amps)	B	175	225
Welding speed (mm/min)	C	150	180
Pulse frequency (Hz)	D	4	8

Table 3. Variables Persistent range

Processing Variable	Constant range
Pulse on time	40 %
Electrode diameter	3.4 mm
Electrode material	97% A + 3% Zr
Purging gas flow rate	8 l/min
Shielding gas flow rate	12 l/min
Pulse ratio	60 %
Filler rod diameter	4 mm

The associations between the quality parameters estimated at different periods during the trials were analyzed using analysis of variance (ANOVA). Using ANOVA, authors learn how much individual process factors and their interactions impact the quality characteristic. The ANOVA can also be used to identify which process variables exhibit the largest standard deviations. Identification and verification of the optimum process parameter setting. The experimental arrangement is shown in Table 4, and the butt joints were made from base metal sheets of 200 × 120 × 4 mm. The sheets of base metal were wire-brushed, degreased with acetone, heated to 100°C, and then pickled in a solution of NaOH and HNO_3. Clamps were used at either end of the sheets to keep them in place, aligned, and with the proper distance between them before welding. There is a purge button at the foot of the bed. The purging and shielding processes have both made use of argon gas. A single welding pass is sufficient to finish the junction.

Table 4. Orthogonal array L8 (27) experimental layout

Exp.no.	**A**	**B**	**C**	**D**

Journal of Physics: Conference Series **2603** (2023) 012039 doi:10.1088/1742-6596/2603/1/012039

1	70	175	150	4
2	70	175	180	8
3	70	225	150	8
4	70	225	180	4
5	80	175	150	8
6	80	175	180	4
7	80	225	150	4
8	80	225	180	8

A tensile test was carried out by removing a piece from the center of each plain and notch joint and milling it to American Society for Testing and Materials (ASTM) E8 specifications. Figure 1a and b demonstrate the two different types of specimens that must be prepared for both the plain and the notch tensile test, respectively. Tensile testing was carried out at a cross head speed of 0.5 mm/min using a standardized, computer-controlled apparatus. Authors could only look at the characteristics of the base metal because all of the welded samples were damaged. Therefore, authors conducted notch tensile strength to expose the weld metal's characteristics.

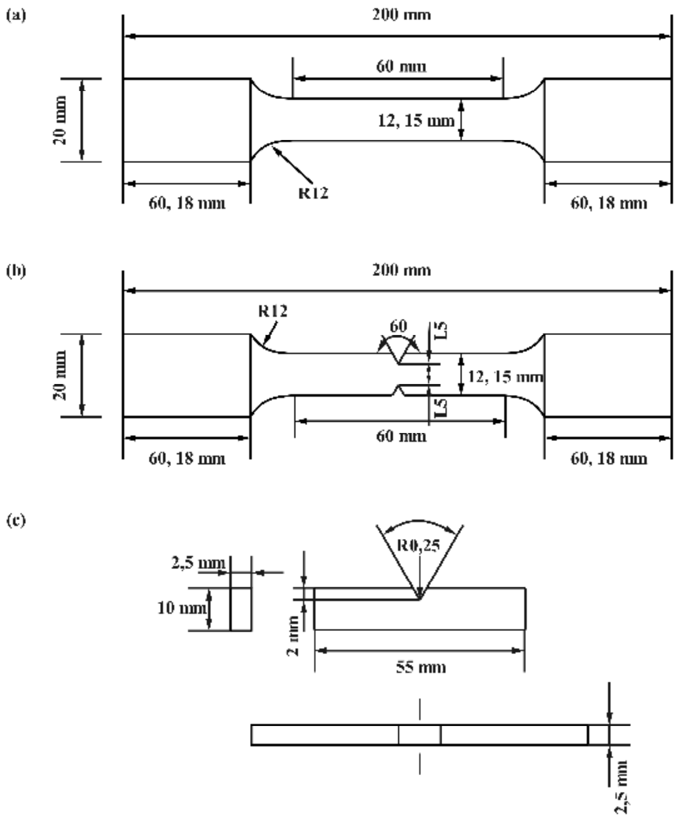

Figure 1. Tensile test specimens in three different configurations: (a) plain, (b) notch, (c) Charpy V-notch

The impact test sample was constructed in accordance with ASTM A370 standards, and then tested using the Charpy impact testing machine. Samples were taken by slicing joints in half for further examination through metallography and micro hardness testing (15 mm in width). Standard metallographic processes, including sectioning, mounting, mechanical polishing, and etching with modified Keller's reagent, were applied to the specimens (2 ml HF, 3 ml HCl, 20 ml HNO_3 and 175 ml H_2O). Welded samples were tested utilizing a Vickers hardness tester at 15 g for 15 s in order to determine their micro-hardness. Micro hardness was evaluated on the welds, HAZ, and unaffected base metal at 0.15 mm, 0.5 mm, and 1mm intervals. The aggregate findings of the hardness analysis are shown in Figure 2.

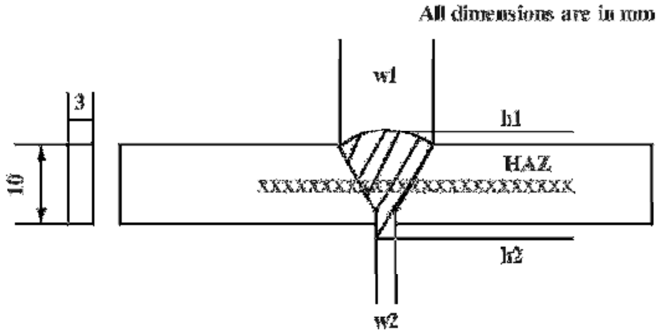

Figure 2. A cross-sectional diagram depicting the transverse hardness test of a weld

After converting the volume proportion of the BM into the weld metal to an area fraction (which is considered to represent volume fraction), authors were able to assess the degree of weld metal dilution.

$$\text{Welding metal dilution (\%)} = \frac{Ab}{Aw} \times 100 \quad (1)$$

Ab = Area of base metal cross section that melted

Aw = Reinforcement of the weld bead's cross-sectional area.

3. Results and discussions

3.1 Mechanical properties

The findings of tests conducted to ascertain the dilution, notch tensile strength, impact energy, hardness of pulsed Tungsten Inert Gas welds is summarized in Table 5. A regression analysis was performed on all of the available data on all of the characteristics and dilution. The suggested regression equations use the factorial space to predict notch tensile strength, impact toughness, hardness, and dilution. Table 6 summarizes regression equations and correlation coefficients for the measured features to emphasize the interdependent effects of the components. The parameters and the data on the observable properties are said to be well-related if and only if the correlation coefficient between them is high. Notch tensile strength grows in tandem with the square of the pulse frequency and the square of the pulse current.

Table 5. The weld mechanical characteristics of Aluminum-Zinc-Magnesium alloys

Sample ID	Notch Tensile Strength (MPa)		Micro-Hardness (HV)		Impact energy (J)		Dilution (%)	
	Test 1	Test 2	Test 1	Test 2	Test 1	Test 2	Test 1	Test 2
1	185	180	81	76	3.0	4.0	85.57	70.45
2	196	191	92	101	3.5	3.0	86.48	84.34

3	178	180	91	96	2.0	2.5	77.26	65.66
4	184	181	95	91	5.0	4.0	80.38	76.65
5	196	197	121	116	2.0	3.0	95.33	86.24
6	191	191	101	106	3.0	3.0	82.55	83.63
7	184	176	103	105	4.0	4.0	72.49	80.23
8	194	191	97	96	5.0	5.0	78.31	80.46
BM	332	335	121	119	2.0	2.1	—	—

Table 6. Equations of regression for mechanical characteristics

S. No.	Response	Regression equation	Coefficient of correlation
1	Notch Tensile Strength	Y=1046 - 11.60 A - 3.450 B - 0.9167 C + 1.625 D + 0.04600 A*B + 0.01333 A*C - 0.02500 A*D	$x_3$0.92
2	Hardness	Y=-1098 + 14.52 A + 3.630 B + 3.683 C - 17.12 D - 0.04500 A*B - 0.04500 A*C + 0.2375 A*D	0.91
3	Impact toughness	Y=- 75.00 + 1.188 A - 0.1200 B + 0.6333 C - 0.5000 D + 0.001500 A*B - 0.009167 A*C + 0.006250 A*D	0.96
4	Dilution	Y= -574.2 + 8.323 A + 1.852 B + 0.6463 C + 28.59 D - 0.02515 A*B - 0.005183 A*C - 0.3889 A*D	0.94

Micro-hardness measurements taken perpendicular to the weld direction revealed four distinct zones on a typical sample 5 weld: the weld center (WC), the heat-affected zone (HAZ), the partially melted zone (PMZ), and the unaffected base metal. The PMZ is stronger than the weld core because the grains in the PMZ are smaller. The HAZ has a lower hardness because of the deformed grains that characterize the region. The weakening precipitates are responsible for the HAZ softening in Aluminium Alloy 5128 [28]. The area immediately adjacent to the weldment is tougher than the remaining of the heat affected zone yet comparatively brittle compared to the base metal due to a long history of solutioning and rapid cooling. Very fine precipitates formed during cooling or natural ageing may account for a local hardness surge around the fusion border. The soft zone is smallest when the percentage by which the actual hardness of the base metal falls short of the predicted value is also smallest (3 mm).

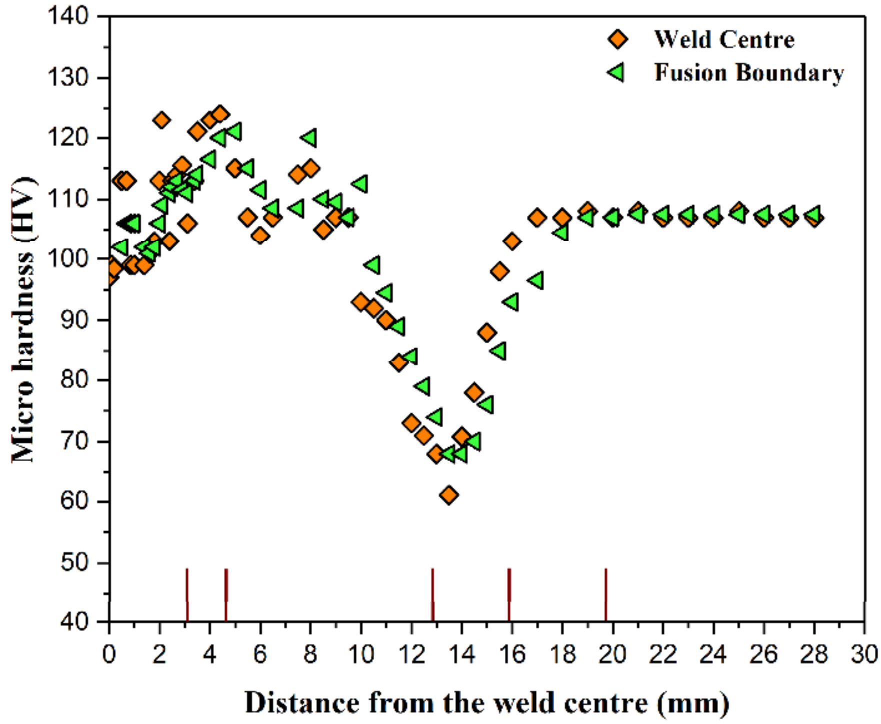

Figure 3. Analyzing the micro hardness of Al-Mg-Si welds in a transverse direction to the weld

3.2 Optimization of processing factor

Taguchi's technique for optimizing process parameters allows for the exploration of the impacts of independent and interacting variables on the given quality attributes; in this case, notch tensile strength, hardness, impact toughness, and dilution. Table 7 displays the best outcomes. The average findings from trials performed under optimal conditions and the evaluation of mechanical properties are shown in Table 8. The experimental values are found to be much more in line with the optimal ones.

Table 7. Optimal range of the superiority attributes

Quality attributes	Optimal level	Optimal range
Notch Tensile Strength (MPa)	A2B1C2D2	195
Hardness (HV)	A2B1C2D2	110
Impact toughness (J)	A1B2C2D1	2.5
Dilution (%)	A2B1C2D2	80.25

Table 8. Validation of the optimum outcomes

Quality attributes	Optimum condition	Optimum value	*Experimental value
NTS (MPa)	A2B1C2D2	195	192.56
Hardness (HV)	A2B1C2D2	110	108.25
Impact toughness (J)	A1B2C2D1	2.5	3.25
Dilution (%)	A2B1C2D2	80.25	78.56

* Average of three values

The analysis of variance revealed that the base current, pulse frequency, and peak current strongly impacted all quality measures. Figure 4 shows a visual representation of the effect that process factors and their interplay have on quality attributes. Figure 4a-c demonstrates that the pulse frequency is second in importance to the base current given in determining dilution and mechanical qualities. Incorporating more of the BM into the weld is crucial for enhancing the grain structure, since the best results are accomplished by a combination of notch tensile strength and dilution [29]. Pulsed Tungsten Inert Gas welding has had its effect on metal characteristics investigated. These findings suggest that P5 (using a 200 A peak current, 60 A base current, 150 mm/min weld speed, and 6 Hz pulse frequency) yielded the finest equiaxed grains in the welded samples. There is a fine inter-dendritic network of aluminum, and the Mg_2Si eutectic largely precipitates near the dendrite borders. Using image analysis software, authors found that the volume of Mg_2Si eutectic, as defined by ASTM E 562, was greater in the weld condition sample 5. The precise value was 28.27%. It has been hypothesized that heat and mechanical disturbances are more perceptible at higher frequencies because their resonance frequency is nearer to the experimented frequency of process (6 Hz). There are echoes of this trend elsewhere in the literature. The sample 4 condition set, when examined up close, showed evidence of coarse grain structure (using a 200 A peak current, 60 A base current, 150 mm/min weld speed, and 6 Hz pulse frequency). It was discovered that condition P4 had the lowest volume percentage of the Mg_2Si eutectic phase (i.e., 10.28 %). At lower frequencies, thermal and mechanical disturbances may be predicted to be smaller. The microstructure of the weld shows that the base current, the peak current, and the pulse frequency all worked together to create the tiny equiaxed grain structure [30-32].

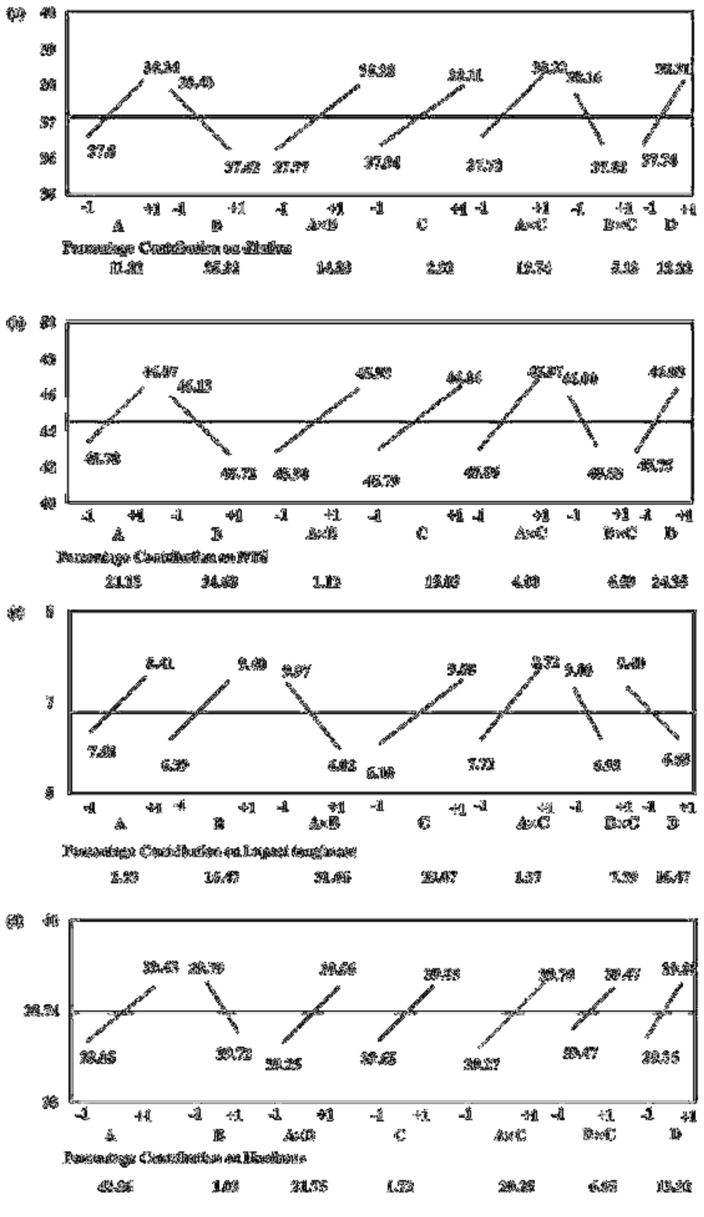

Figure 4. Signal-to-noise ratio (SNR) and contribution percentage (%) of variables and its interactions (shown graphically). (a)Microhardness, (b) Aluminium Alloy, (c) Impact Resistance, (d) Dilution

4 Conclusions

Both notch tensile strength and diluting effects can be maximized with the appropriate combination of elements, A2B1C2D2. Weld behavior changes at the best possible set of process variables because more base metals are diluted into the weld, leading to more Mg_2Si precipitates being generated in the aluminium matrix. Also, the study shows that the weld center has a fine grain structure, which leads to improved mechanical qualities. However, a coarse grain structure explains why the impact toughness optimal combination is different. The sample 5 parameters yield a rather narrow protected area.

Causes include variations in welding technique, cooling rate, dissolution, precipitate development, and the generation of stable phases. Within the specified range of parameters, regression models were created to predict the quality features.

References

[1] Akopyan T K *et al.,* 2013, *Russ. Metall* **7** 545.
[2] Zhang H *et al.,* 2019 *J. Mater. Eng. Perform* **28** 1790.
[3] Gonchikar U *et al., 2019 ASME International Mechanical Engineering Congress and Exposition, Proceedings (IMECE).*
[4] Song Q *et al.,* 2019 *Adv. Eng. Mater* **21**.
[5] Assefa A T *et al.*, 2022 *Materials (Basel)* **15**.
[6] Sivachidambaram P *et al.,* 2015 *Indian J. Sci. Technol* **8**.
[7] Moi S C *et al.,* 2019 *Int. J. Recent Technol. Eng* **8** 5348.
[8] Dey H C *et al.,* 2013 *Weld. World* **57** 903.
[9] Skariya P D 2019 *Int. J. Nano Biomater* **8** 277.
[10] Linger M A 2023 *et al., Eng. Res. Express* **5**.
[11] Zhang G *et al.,* 2016 *Hanjie Xuebao/Transactions China Weld. Inst* **37** 105.
[12] Pamnani R *et al.,* 2017 *Trans. Indian Inst. Met* **70** 49.
[13] Benlamnouar M F *et al.*, 2019 *Solid State Phenom* **297** 51.
[14] Nageswara Rao K *et al.,* 2018 *Int. J. Mech. Prod. Eng. Res. Dev* **8** 659.
[15] Chuaiphan Wand L *et al.,* 2020 *J. Manuf. Process* **58** 163.
[16] Anuradha M *et al.,* 2021 *Materials Today: Proceedings* **52** 1314.
[17] Srinivasan G *et al.,* 2011 *Fusion Eng. Des* **86** 446.
[18] Ceschini L *et al.,* 2010 *Metall. Ital* **102** 23.
[19] Patil H S *et al.,* 2019 *Frat. ed Integrita Strutt* **13** 377.
[20] Ghumman K Z *et al.,* 2022 *J. Mater. Res. Technol* **21** 220.
[21] Benlamnouar M F *et al.,* 2021 *Lecture Notes in Mechanical Engineering* 463.
[22] S. Kumar *et al.*, 2020 *Materials Today: Proceedings* **22** 3181.
[23] Srinivasan L *et al.,* 2017 *Materials Today: Proceedings* **4** 8874.
[24] Irechukwu C C *et al.,* 2021 *Weld. Int.*, **35** 45.
[25] Thang S M *et al.,* 2021 *Lecture Notes in Mechanical Engineering* 152.
[26] Chandrasekar G *et al.,* 2017 *Trans. Indian Inst. Met* **70** 671.
[27] Park J C *et al.,* 2011 *Rare Met* **30** 628.
[28] Girimurugan R *et al.,* 2023 *Materials Today: Proceedings* 74 602.
[29] Vairavel M *et al.,* 2020 *AIP Conference Proceedings* **2283** 020112.
[30] Anandha Moorthy A *et al., 2021 Advances in Materials Research: Select Proceedings of ICAMR* 629.
[31] Pradeep G M *et al.,* 2022 *Materials Today: Proceedings* **56** 3196.
[32] Girimurugan R *et al.,* 2022 *ECS Transactions* **107** 7381.